Available online at www.sciencedirect.com
SCIENCE DIRECT®
Pergamon
Acta Materialia 51 (2003) 3429–3443
Acta MATERIALIA
www.actamat-journals.com

Deformation behavior of the $Zr_{41.2}Ti_{13.8}Cu_{12.5}Ni_{10}Be_{22.5}$ bulk metallic glass over a wide range of strain-rates and temperatures

J. Lu [a], G. Ravichandran [a,*], W.L. Johnson [b]

[a] *Graduate Aeronautical Laboratories, California Institute of Technology, Pasadena, CA 91125, USA*
[b] *W.M. Keck Laboratory of Engineering Materials, California Institute of Technology, Pasadena, CA 91125, USA*

Received 15 November 2002; received in revised form 9 March 2003; accepted 12 March 2003

Abstract

The stress-strain relations for the $Zr_{41.2}Ti_{13.8}Cu_{12.5}Ni_{10}Be_{22.5}$ bulk metallic glass (Vitreloy 1) over a broad range of temperatures (room temperature to its supercooled liquid region) and strain rates (10^{-5} to 10^{3} s^{-1}) were established in uniaxial compression using both quasi-static and dynamic Kolsky (split Hopkinson) pressure bar loading systems. Relaxation and jump in strain rate experiments were conducted to further understand the time dependent behavior of Vitreloy 1. The material exhibited superplastic flow above its glass transition temperature (623 K) and strain rates of up to 1 s^{-1}. The viscosity in the homogeneous deformation regime was found to decrease dramatically with increasing strain rate. A fictive stress model was used to describe the basic deformation features of Vitreloy 1 under constant strain-rate loading as well as multiple strain-rate loading at high temperatures.

Keywords: Bulk amorphous materials; Metallic glasses; Compression test; High temperature deformation; Superplasticity

1. Introduction

Progress made in the last few decades has shown that metastable glassy metals can be formed in binary, ternary and multi-component alloy systems (e.g., [1,2]). Atoms of different metals can be kinetically constrained or frozen by rapid quenching techniques such that no long-range order exists in the as processed alloy systems. Following the discovery of a binary Au-Si amorphous alloy in form of thin ribbon using very high cooling rate of 10^5–10^6 K/s [3], the early search for bulk glass forming alloys dated back to the 70s, when several ternary metallic glass formers were found such as Pd-Ni-P [4] and Pd-Cu-Si [5], with dimensions in the millimeter scale. The late 80s and early 90s witnessed a revolution in the development of bulk metallic glasses with lower cooling rates resulting in larger sizes and thus making them attractive candidates for many structural applications [6–10].

Among these new bulk glass forming metallic alloys, a Zr-based material, $Zr_{41.2}Ti_{13.8}Cu_{12.5}Ni_{10}Be_{22.5}$ (Vitreloy 1), exhibits high resistance

* Corresponding author. Tel.: +1-626-395-4525; fax: +1-626-449-6359.
E-mail address: ravi@caltech.edu (G. Ravichandran).

1359-6454/03/$30.00 © 2003 Acta Materialia Inc. Published by Elsevier Science Ltd. All rights reserved.
doi:10.1016/S1359-6454(03)00164-2

with respect to crystallization in its wide supercooled liquid region. It is processed at low cooling rate of around 1 K/s [7] and can be cast up in sizes of up to 2 to 4 cm in thickness. The high yield stress [10,11] and the high strength to density ratio of this bulk metallic glass makes the material an excellent candidate for structural applications. Research on its viscosity, relaxation, kinetics and crystallization [12–15] has shown that thermo-mechanical characterization up to its crystallization temperature is made possible by the increased thermal stability of the glassy alloy with respect to crystallization.

Generally speaking, the deformation of metallic glasses can be classified into two modes, namely, homogeneous and inhomogeneous deformation. In spite of their metallic bonding, all the metallic glasses discovered so far exhibit shear localization at room temperature, leading to catastrophic shear failure immediately following yield. At higher temperatures, they can be deformed homogeneously, exhibiting considerable amount of inelastic deformation. Recently, homogeneous deformation of several metallic glasses around their glass transition temperature was investigated, including the tensile deformation of 20 μm thick $Zr_{65}Al_{10}Ni_{10}Cu_{15}$ ribbons [16] and 40 μm thick $La_{55}Al_{25}Ni_{20}$ ribbons [17]. The use of ribbons instead of their bulk forms in millimeter scale was probably due to limitations in the availability of materials and the experimental setup. In these investigations, necking appears during most tensile tests, making the observation of variation of the steady state stress difficult. Experiments on bulk $Zr_{55}Al_{10}Ni_5Cu_{30}$ specimens of 3 mm in diameter [18] and bulk $Pd_{40}Ni_{10}Cu_{30}P_{20}$ specimens of 2 mm in diameter [19] have been performed in their homogeneous deformation regime. The strain rate was limited to the quasi-static range and the temperature in the vicinity of the corresponding glass transition temperature. Recently, Nieh et al. [20] investigated the plasticity and localization of the bulk amorphous $Zr_{52.5}Al_{10}Ti_5Cu_{17.9}Ni_{14.6}$ alloy in its supercooled region. They attributed the non-Newtonian behavior observed during deformation to the formation of nanocrystallites during the high temperature deformation.

There exist a number of theories to describe the deformation behavior of metallic glasses. Argon developed a model based on the idealization of two deformation modes, namely the diffuse shear transformation and the dislocation loop formation, to analyze the boundary between homogeneous and inhomogeneous flow of Pd-Si metallic glass [21–23]. Spaepen proposed a theory based on the free volume created by external stress and its annihilation by diffusion [24]. This was further modified by Steif et al. to analyze mechanical deformation problems by including additional free volume change due to pressure [25]. Khonik suggested a directional structural relaxation model, which states that each rearrangement event can be interpreted as a thermally activated shear due to local atomic structures and subsequently nearly athermal viscous flow by external stress [26]. Among these models, Speapen's free volume based model seems to be the most widely cited to interpret the deformation behavior of metallic glasses. Duine used the free volume based viscosity assumption by Speapen and defect evolution assumption to analyze the kinetic process of defects and their steady state concentration [27]. de Hey et al. applied the same idea to temperature induced structural evolution of some metallic glasses, leading to the conclusion that additional free volume is created as compared with thermal equilibrium due to plastic deformation [28–30]. Recently, Kato and Chen et al. adopted a simple model based on the concept of fictive stress to simulate stress-strain behavior of metallic glasses [31,32], which will be discussed in detail later.

Deformation of bulk metallic glass differs from that of a crystalline metallic material due to the absence of long-range order, i.e., amorphous in nature. Relatively little is known regarding the effect of rate and temperature on the deformation behavior of Vitreloy 1, particularly in the supercooled liquid region. The objective of this study is to systematically explore the thermo-mechanical behavior of the $Zr_{41.2}Ti_{13.8}Cu_{12.5}Ni_{10}Be_{22.5}$ (Vitreloy 1) bulk metallic glass under uniaxial compression subject to a wide range of strain rates and temperatures. Compression loading was chosen in the present study because tensile loading typically induces necking at relatively small strains while compression can result in uniform defor-

mation up to large strains provided care is used in conducting the experiments. The experimental results can aid in the development of appropriate constitutive models and delineate possible deformation modes for bulk metallic glasses over such a wide range of temperatures and strain rates. Such constitutive models are expected to provide design rules for processing and structural applications of bulk metallic glasses. In addition, they may be also employed in the design of a new generation of high-pressure casting facilities and net-shape forming thermomechanical processes for structural amorphous metals.

2. Experimental

The bulk metallic glass used in this investigation is $Zr_{41.25}Ti_{13.75}Cu_{12.5}Ni_{10}Be_{22.5}$ with the commercial name Vitreloy 1 (commonly referred to as Vit 1). Vitreloy 1 is the trademark (™) name used by Liquid Metal Technologies, Inc., Laguna Niguel, CA, for the afore mentioned bulk metallic glass. The processing, physical and mechanical properties of this material are well documented in the literature (see for example, [7,10–13,15,33–36]). Relevant thermo-physical and mechanical properties of Vitreloy 1 are given in Tables 1 and 2. The as-received samples were examined using X-ray diffraction and the presence of broad diffuse peaks and lack of discrete peaks revealed that the as-received material is amorphous. Differential scanning calorimetry (DSC) study of the as-received material revealed that the temperatures at the onset of the glass transition and at the onset of the crystallization are 623 and 710 K, respectively when subject to a heating rate of 20 K/min.

Table 2
Physical and mechanical properties of $Zr_{41.2}Ti_{13.8}Cu_{12.5}Ni_{10}Be_{22.5}$ at room temperature

Property	Value
Density (kg/m^3)	6,000
Young's modulus (GPa)	96
Poisson's ratio	0.36
Elastic strain limit	0.02
Tensile yield strength (GPa)	1.90
Vickers hardness (kg/mm^2)	534

The Vitreloy 1 specimens used in this investigation had a typical cross section of 3.7×3.7 mm and a nominal length-to-width aspect ratio of 2:1 and 1:1 in the quasi-static and the dynamic experiments, respectively. The quasi-static experiments were carried out using a screw-driven Instron (model #4024) system with a 50 kN load cell and a servo-hydraulic Materials Testing System (MTS with a 319 series axial/torsional load frame and 358 series load units). The strain rate achieved using these systems for the size of the specimens employed ranges from 10^{-5} to 10^{0} s^{-1}. The strain measurement was carried out by recording the relative displacement of the end surfaces of the two push rods using a Linear Variable Differential Transformer (LVDT, Schaevitz model #050-MHR) with an output sensitivity of around 2–3 mV/micron displacement. To accomplish the displacement measurement, an extension-rod mini-apparatus was designed and the details of which can be found elsewhere [37]. The high strain rate experiments were carried out using a Kolsky (split Hopkinson) pressure bar apparatus [38–40]. Certain modifications, such as pulse shaping and single loading, were adopted in using the Kolsky

Table 1
Thermodynamic and kinetic properties of $Zr_{41.2}Ti_{13.8}Cu_{12.5}Ni_{10}Be_{22.5}$ (Vitreloy 1)

Property	Condition	Value	Reference
Onset glass transition temperature (K)	Heating rate, 20 K/min	623	[7]
Onset of first crystallizationtemperature (K)	Heating rate, 20 K/min	705	[7]
Supercooled liquid region (K)	Heating rate, 20 K/min	80	[7]
Liquidus temperature (K)		993	[7]
Viscosity (Pa-s)	Melting temperature	2–5	[13]

pressure bar for the investigation of high strength and quasi-brittle materials such as bulk metallic glasses [37,40,41]. The strain rate achieved using this system for the size of the specimens employed ranges from 10^2 to 10^3 s^{-1}.

A temperature control system with a resolution of ±0.5 K was designed and used in this study [37]. The temperature at which the experiments were performed ranged from room temperature (295 K) to the supercooled liquid region of Vitreloy 1. It is not surprising that a slight change in the glass transition temperature T_g with respect to heating rate was observed, indicating that the T_g is not a unique physical property of the glass, but rather a thermal-history dependent kinetic quantity. In order to diminish the influence due to the variation of heating rate on the thermal history of the specimens during mechanical loading, the specimen was constantly heated at a fixed heating rate of 20 K/min until a desired temperature was reached. Subsequently, the specimen was held at the desired temperature for 3–10 min prior to loading. The temperature then kept unchanged during the course of compression.

Since the present study attempts to investigate the effects of temperature on flow in detail, the following set of temperatures was selected: 295 (room temperature), 373, 423, 473, 523, 573, 593, 603, 613, 623 (the glass transition temperature of Vitreloy 1), 643, 663 and 683 K. The TTT (time-temperature transformation) diagram for Vitreloy 1 [12] exhibits a nose-shaped temperature-time crystallization behavior. The presence of phase separation and primary crystallization event occurs at approximately 1000 s at 683 K and at more than 10,000 s at 600 K, providing sufficient operational time windows for conducting the compression experiments. The use of the TTT diagram was based on the assumption that the stress-driven material phase change is negligible compared with annealing. Although stress-driven free volume creation has been reported by other researchers [29], to the author's knowledge, no observation on the stress-driven phase separation has been reported in the literature, but this remains an interesting topic for further study.

Compression experiments at even higher temperatures were also attempted. However, the relatively low viscosity and possible rapid crystallization at these temperature levels, 703 K and above made the experiments uncontrollable and unreliable (also, there was a negligible, yet persistent initial permanent stress due to the measurement method). Therefore, all the experiments presented in this study will be confined to the temperature range of 293–683 K.

The stress and strain quantities presented here are "true" stress and "true" (logarithmic) strain data. One problem in making a definitive statement as to whether the concepts of true strain and stress are valid for metallic glasses is related to the volumetric deformation of the amorphous system, which consists of both atoms and associated unoccupied free volume [24]. The latter plays an important role from a statistical point of view in assisting atomic arrangements driven by external forces and/or thermal energy: even a tiny change of the free volume could induce a dramatic variation in the flow behavior [25]. The study by Masuhr et al. [14] provides a value for the normalized free volume in Vit 1 to be approximately 3% around the glass transition temperature and in the supercooled liquid region. However, no data on free volume variation due to large mechanical deformation is readily available in the literature. However, the result for $Pd_{40}Ni_{40}P_{20}$ metallic glass [29] shows that the normalized free volume changed from 3.1 to 3.4% after a uniaxial deformation to a strain of 0.11 at 556 K and a strain rate of 1.7×10^{-4} s^{-1}. As the free volume has negligible influence on volume change during deformation, the adaptation of true measures of strain and stress in the present study appears reasonable. Further study of the compressibility of metallic glasses under thermomechanical loading is needed.

3. Results

3.1. Effect of temperature on stress-strain behavior

The influence of temperature on failure modes is one of the key features of deformation of materials and their characterization, i.e., brittle to

ductile transition. A typical example of the stress-strain curves is shown in Fig. 1 for a strain rate of $1.0 \times 10^{-1}s^{-1}$. To clearly distinguish each stress-strain curve while presenting all of them in the same plot, some of the curves were shifted along the strain axis by a strain value in the range of 0–0.02. As shown in Fig. 1, Vitreloy 1 exhibited a high failure stress of 1860 MPa at room temperature and failed by the formation of a single shear band and subsequent shear fracture. As the temperature was increased to 373 K, the maximum stress decreased slightly to 1790 MPa. This general trend of the decrease in the maximum stress continued a temperature between 643 and 663 K, where the deformation mode switched from being inhomogeneous (shear failure) to being homogeneous.

In the temperature range of 663–683 K, deformation remained homogeneous up to the strain value demonstrated on each curve. The term "homogeneous deformation" as used here means uniform deformation of the specimen at a macroscopic scale, i.e., shape and size of the cross-sections of the deforming specimen change simultaneously everywhere along the loading axis, remaining self similar, and no macroscopic shear localization is observed. The counterpart of the homogeneous deformation is the catastrophic shear failure triggered by a major shear band propagation, which is referred to as "inhomogeneous deformation". The maximum strain value of each curve in presenting homogeneous deformation data was merely chosen for convenience in each experiment since there were no indications of any possible impending catastrophic failure. The stress-strain curves in the homogeneous deformation region featured an increase of the initial slope as the temperature decreased, which indicates that the initial Young's modulus (or shear modulus) decreases with temperature, analogous to a similar effect in crystalline metallic alloys. Stress overshoot, the difference between peak stress and flow stress, was present at a temperature of 663 K. The cause of the stress overshoot was due to the free volume induced structural relaxation [24], which will be discussed in detail in the following section. At 683 K, the stress increased monotonically as the strain increased until it reached a steady state value and subsequently leveled off as the strain increased further. The temperature sensitivity is much larger compared with traditional crystalline metallic alloys since the steady state stress decreased by over 50% as the temperature increased by 20 K over 663 K.

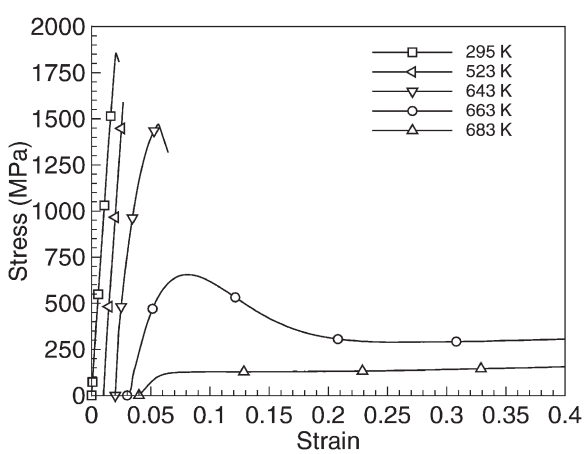

Fig. 1. Effect of temperature on the uniaxial stress-strain behavior of Vitreloy 1 at strain rate $\dot{\varepsilon} = 1.0 \times 10^{-1}\ s^{-1}$ and temperatures T = 295, 523, 643, 663 and 683 K. The stress-strain curves have been shifted to the right to avoid overlapping curves of similar shapes and sizes.

3.2. Effect of strain rate on stress-strain behavior

In addition to the strong temperature dependence of the deformation of Vitreloy 1, the strain rate dependence of the stress-strain curves was also investigated. Two typical dynamic strain rates, $2.5 \times 10^{2}\ s^{-1}$ and $1.0 \times 10^{3}\ s^{-1}$, were chosen for the Kolsky bar experiments to investigate the material behavior in the same temperature range as in the quasi-static experiments.

Fig. 2 illustrates an example of the stress-strain curves obtained at temperature of 643 K for strain rate in the range of $1.0 \times 10^{-4}\ s^{-1}$ to $1.0 \times 10^{3}\ s^{-1}$. It was found that shear localized failure characterized the deformation mode at higher strain rates ranging from $1.0 \times 10^{-1}s^{-1}$ to $1.0 \times 10^{3}s^{-1}$. The stress-strain curves at higher strain rates have a linear slope until failure and no inelastic post-yielding was evident. After reaching the maximum stress, the stress dropped to its zero

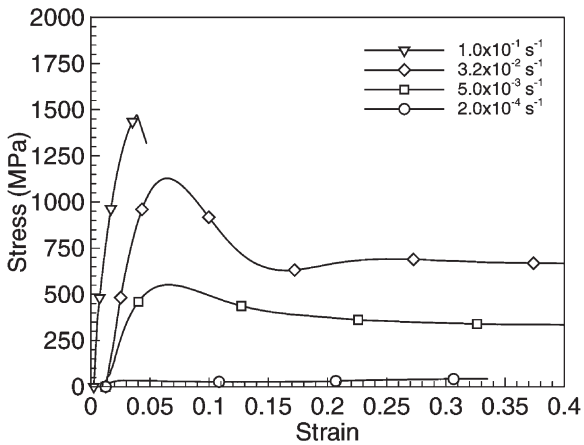

Fig. 2. Effect of strain rate on the uniaxial stress-strain behavior of Vitreloy 1 at temperature $T = 643$ K and strain rates of 1.0×10^{-1}, 3.2×10^{-2}, 5.0×10^{-3} and 2.0×10^{-4} s^{-1}. The stress-strain curves have been shifted to the right to avoid overlapping curves of similar shapes and sizes.

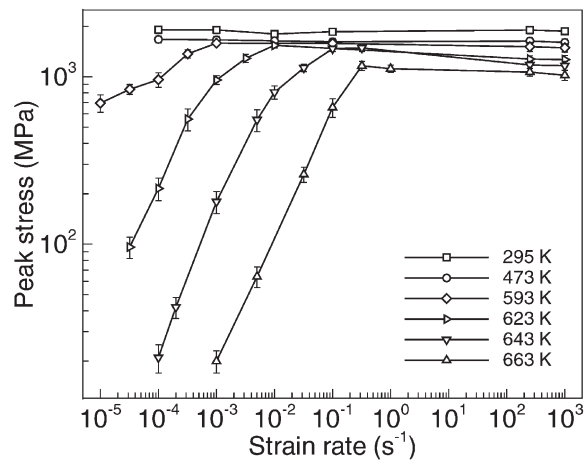

Fig. 3. Plot of the peak stress as a function of strain rate at various temperatures.

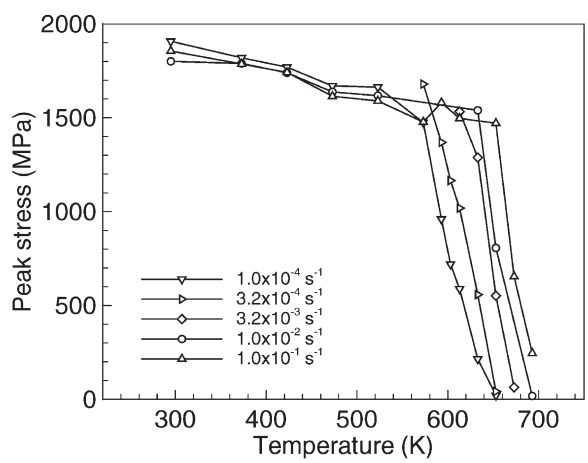

Fig. 4. Plot of the peak stress as a function of temperature at various strain rates.

value immediately, typical of "brittle" failure. The failed surface exhibited a "vein-like" pattern on each of the recovered specimens. The general tendency is that the maximum stress decreased slightly with increasing strain rates, as will be summarized later. It is clear that increase in strain rate led to a transition from homogeneous flow to inhomogeneous deformation. Therefore, the effect on the stress-strain curves due to a decrease in strain rate is similar to that due to increase in ambient temperature, as depicted in Fig. 1.

3.3. Peak stress and overshoot stress

The peak stress, one of the principal parameters that characterize the strength of the bulk metallic glass, is plotted as a function of strain rate and temperature in Figs. 3 and 4, respectively. In the homogeneous deformation region, the peak stress variation is quite similar to that of the steady state stress, discussed later. Both these stress quantities have pronounced dependences on strain rate and temperature. On the other hand, the variation of the peak stress with respect to strain rate and temperature in the inhomogeneous region is quite small compared to its variation in the homogeneous region. The average peak stress was reduced from around 1850 MPa at room temperature to about 1570 MPa at about 573 K. However, a remarkable drop in peak stress occurred at higher temperatures. For instance, at the strain rate of $1.0 \times 10^{-4}s^{-1}$, the peak stress dropped from 1475 MPa at 573 K to about 21 MPa at 653 K, by a factor of 70 for a change in temperature of only 80 K. These results suggest that Vitreloy 1 should not be used in applications where ambient temperature is substantially higher than 573 K, which can be regarded a threshold temperature beyond which this metallic glass cannot be employed as a structural material, but

could be viewed as the temperature above which it can be processed or cast into net shape easily.

The magnitude of stress overshoot with respect to strain rate and temperature is plotted in Fig. 5. The overshoot stress increased monotonically as the strain rate increased, and increased with decreasing temperature. This clearly illustrates the opposing roles played by strain rate and temperature on the deformation and failure modes of Vitreloy 1.

3.4. Relaxation

Preliminary experiments on the relaxation behavior of Vitreloy 1 were conducted at ambient temperatures of 593, 613, 623 and 643 K. A specimen was uniaxially compressed to a certain strain level at a prescribed strain rate selected for each temperature and held fixed at that strain level. The strain levels were chosen such that the corresponding initial stress (σ_0) is lower than its steady state flow stress. The stress relaxation was then recorded as a function of time using the load cell data. The data for the normalized stress, σ/σ_0, where σ is the stress during the relaxation and σ_0 is the stress at the beginning of the relaxation, are shown in Fig. 6(a) as a function of time. If the relaxation time is denoted by the time when $\sigma/\sigma_0 = 1/e$ (0.368), then the relaxation time are 21.5, 327, 1530 and 5920 s at temperatures of 593, 613, 623 and 643 K respectively (see Fig. 6(b)).

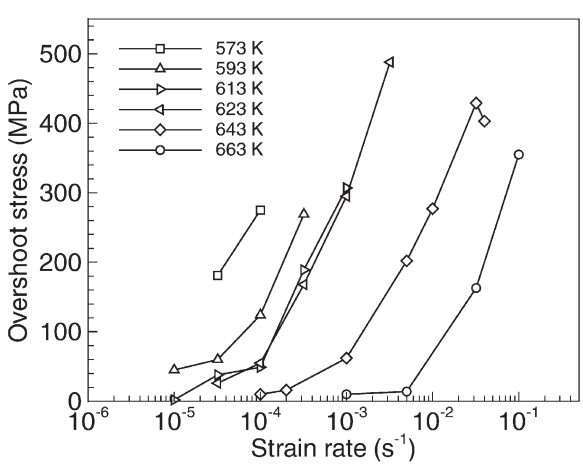

Fig. 5. Overshoot stress as a function of strain rate at various ambient temperatures.

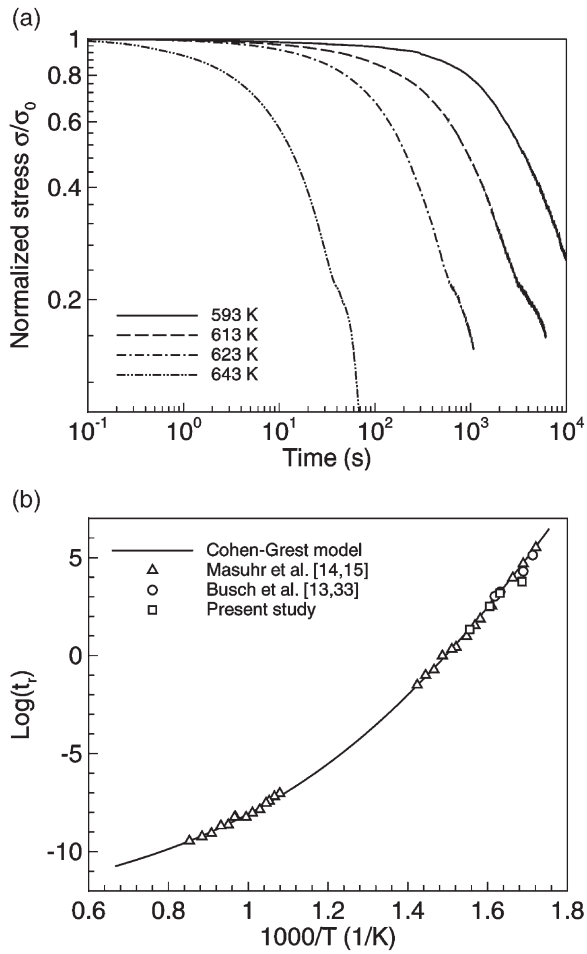

Fig. 6. (a) Plot of the normalized stress as a function of time at various ambient temperatures. (b). Plot of relaxation time as a function of reciprocal temperature.

4. Discussion

4.1. Effects of strain rate and temperature on viscosity

At sufficiently low temperatures, metallic glass behaves like a typical brittle solid material. To process such a material, it is necessary to heat it to a temperature at which it either softens or melts to undergo a shape change operation. Thus, the ability

to measure and characterize the viscosity of a metallic glass is important for optimizing its processing conditions. Among all fluids, a Newtonian fluid has the simplest constitutive behavior, in which the strain rate is directly proportional to the stress. However, some fluids exhibit a non-linear (i.e., non-Newtonian) response to shearing stress, where viscosity is a shear rate dependent quantity. Polymeric fluids, such as melts and solutions, are often non-Newtonian [42]. The physical similarity between the amorphous structure of metallic glasses and glassy polymers suggests that metallic glasses at higher temperature exhibit behavior similar to that of polymers. For Vit 1 metallic glass at high temperatures, the characterization of its flow behavior has been limited to the Newtonian range [14,15]. In this section, the variation of viscosity (i.e., shearing viscosity) with strain rate will be studied, where the shearing viscosity is deduced from the experimental data as one-third of the ratio of the steady state stress to the corresponding uniaxial strain (loading) rate [43,44].

The values of steady-state flow stress are plotted in Fig. 7 with respect to strain rate at various temperatures. The steady state stress for a given temperature increases linearly with strain rate at lower strain rates. At higher strain rates, a non-linear effect appeared, featuring a bending-over of the stress-strain rate curves, i.e., the rate of the increase in steady state stress decreased as the strain rate increased. This effect is manifested by the strain rate and temperature dependence of the viscosity shown in Fig. 8. At strain rates lower than some specific value for each temperature, the viscosity remained essentially unchanged or changed very little, within the experimental error. Although it was not easy to observe this phenomena at relatively low temperatures using the current compression setup and loading system, steady state viscosities at lower strain rates and temperatures of 573, 593, 603 and 613 K can be obtained using the three point beam bending apparatus [14,15]. Higher strain rates, however, led to a remarkable decrease in the viscosity for temperatures in the range of 573–683 K, indicating that the flow is transitioning from Newtonian to non-Newtonian behavior. The experimental results clearly show that stress overshoot accompanies all the stress-strain curves in the non-Newtonian homogeneous deformation regime. In the linear Newtonian regime, internal structural relaxation of the material is fast enough to keep up with the external loading rate, resulting in a monotonically increasing stress-strain curve.

As demonstrated in Fig. 9(a), a master curve (relation) can be constructed for the steady-state flow stress of Vitreloy 1 with respect to normalized strain rate $\dot{\varepsilon}\,\eta_N$, which is the product of Newtonian viscosity η_N and imposed strain rate $\dot{\varepsilon}$. Likewise, a master curve (relation) in terms of viscosity ratio

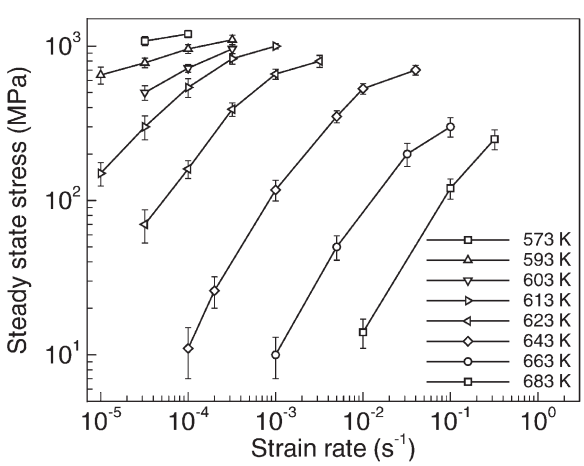

Fig. 7. Steady state stress as a function of strain rate at temperatures T = 573, 593, 603, 613, 623, 643, 663 and 683 K.

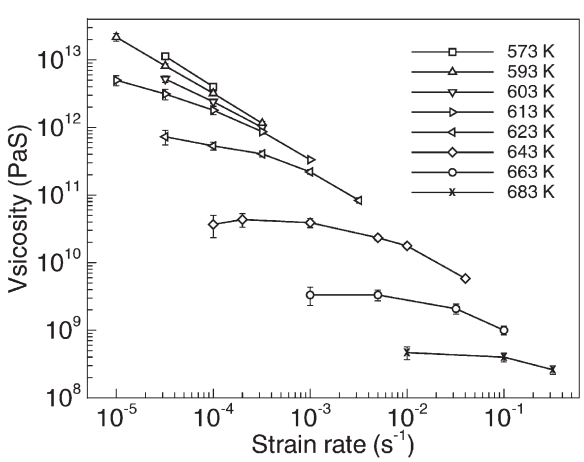

Fig. 8. Viscosity as a function of strain rate at temperatures T = 573, 593, 603, 613, 623, 643, 663 and 683 K.

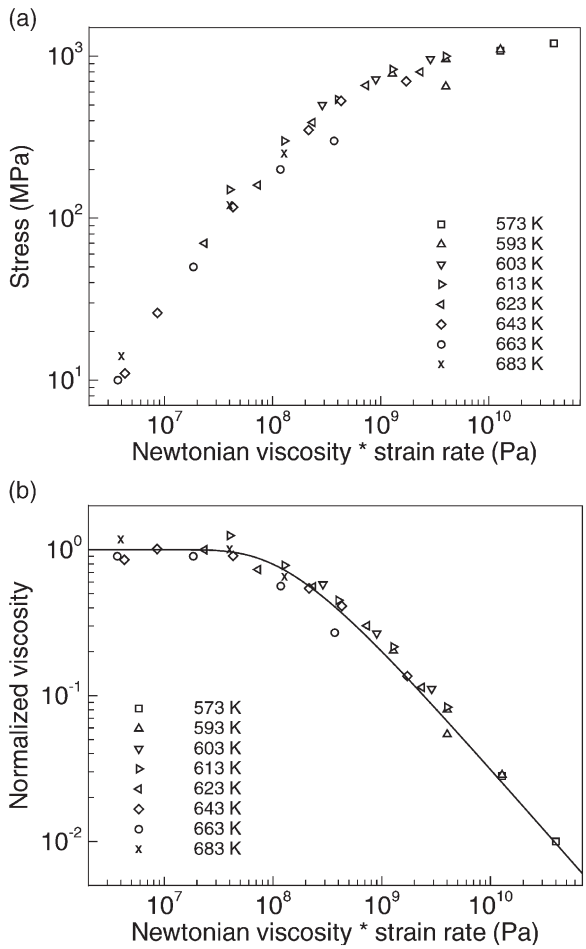

Fig. 9. (a) Steady state stress as a function of strain rate at temperatures T = 573, 593, 603, 613, 623, 643, 663 and 683 K. (b). Normalized viscosity as a function of strain rate at temperatures T = 573, 593, 603, 613, 623, 643, 663 and 683 K.

η/η_N and the normalized strain rate can also be generated, as shown in Fig. 9(b). The master curve describing the viscosity can be expressed in the form (e.g., [42]),

$$\eta/\eta_N = 1-\exp\left(-\left(\frac{\alpha}{\dot{\varepsilon}\ \eta_N}\right)^{\beta}\right) \quad (1)$$

where α and β are fitting parameters for the experimental data. For Vitreloy 1, the values of α and β are 172 MPa and 0.85 respectively and were obtained by fitting the current experimental data. η_N is the Newtonian viscosity which can be described by a free volume model [14],

$$\eta_N = \eta_0\exp(b\ \nu_m/\nu_f) \quad (2)$$

where ν_f is the temperature dependent average free volume per atom according to the Cohen and Grest model [45], $b\nu_m$ is the critical volume for the glass flow and η_0 is a fitting parameter having the units of viscosity. The values of $b\nu_m$ and η_0 were given by Masuhr et al. [14] for Vitreloy 1. The Newtonian viscosity, i.e., the equilibrium viscosity, is also shown in Fig. 10.

Eqs. (1) and (2) can be used to fully determine the viscosity within the homogeneous region; however, they cannot predict the onset of shear localization.

4.2. Homogeneous and inhomogeneous deformation

As described in the previous sections, the deformation of Vitreloy 1 can be categorized into two major regions on a deformation map of strain rate versus temperature, one with homogeneous deformation and the other associated with inhomogeneous deformation, the former featuring either Newtonian or non-Newtonian flow while the latter is characterized by linear elastic behavior followed by shear localization. Based on the experimental data from the current investigation, Fig. 11 shows the boundaries for Vitreloy 1 between the three distinct modes of deformation on the flow map. It has

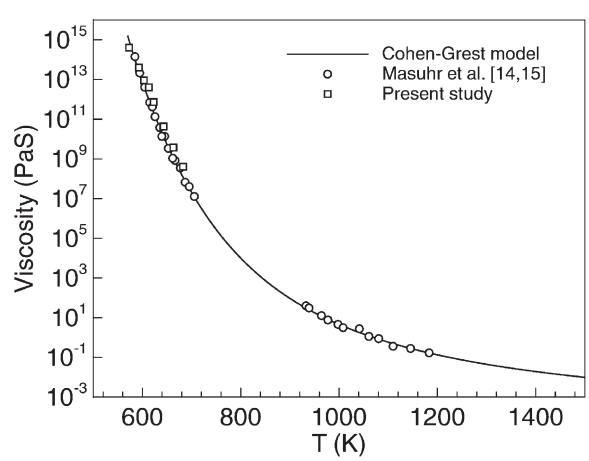

Fig. 10. Equilibrium (Newtonian) viscosity as a function of temperature.

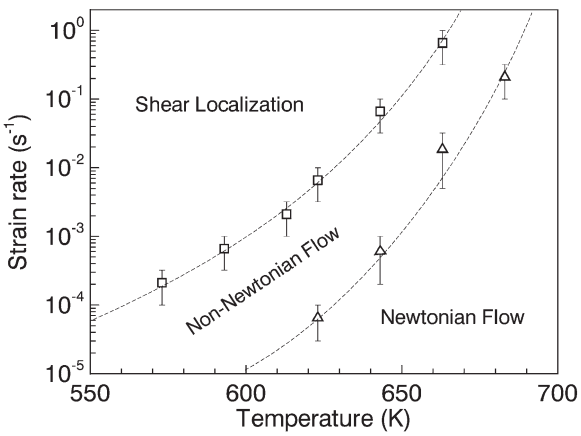

Fig. 11. The boundaries between the three distinct modes of deformation for Vitreloy 1 as determined from the current investigation. Two boundaries are shown in each figure, one for transition from homogeneous deformation to inhomogeneous deformation and the other for transition from Newtonian to non-Newtonian flow.

been realized from all the stress-strain curves that if shear failure occurs in Vitreloy 1, the corresponding failure strain is always less than 5%. The experiments have also confirmed that under uniaxial compressive loading condition, if failure does not occur at the peak stress, Vitreloy 1 will exhibit *superplasticity*, with substantial flow at the corresponding strain rate. Although the peak stress for the onset of shear localization for Vitreloy 1varies with temperature, it is in the range of 1100–1700 MPa.

4.3. Effect of jump in strain rate

The viscous nature of flow and high rate sensitivity of the flow stress of Viterloy 1 during homogeneous deformation allows detailed investigation of the kinetics of flow and associated strength. By varying the strain rate during a uniaxial compression experiment, not only the influence of the preloading history on the steady state can be investigated, but also the effect of the relaxation at the first strain rate on the stress overshoot at the second strain rate can be examined, which provides additional information to further validate flow models for metallic glasses. A series of jump-in-strain-rate experiments was performed where strain rates were abruptly changed from one value to another, while holding the ambient temperature constant. Fig. 12 shows the stress-strain curve where the strain rate was changed from 3.2×10^{-3} s^{-1} to 3.2×10^{-2} s^{-1} (by one order of magnitude) at a strain of around 0.13 at 643 K. The stress-strain curves at 643 K and constant strain rates of 5.0×10^{-3} s^{-1} and 3.2×10^{-2} s^{-1} are also plotted for reference. After the strain rate was changed, the stress-strain curve exhibited a second peak stress which is smaller than the one obtained under constant strain rate loading at the corresponding temperature. This is probably due to the preloading effect that relaxed the glass and/or increased free volume due to inelastic deformation. However, it is obvious that the steady state flow stress was not affected, within the experimental error. In other words, the steady state flow stress is independent of the material deformation history while the overshoot stress does depend on the loading history and the transient response is highly path dependent. Similar observations were made for numerous jump-in-strain-rate tests involving different sequences of strain rates at various temperatures [37].

5. Modeling

In this section, a phenomenological model is employed to describe the flow behavior of Vitreloy

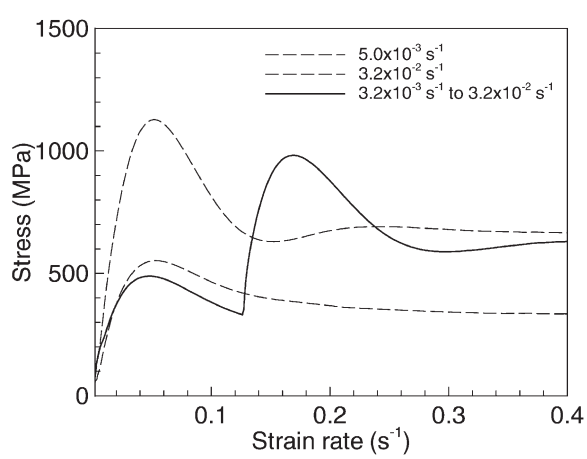

Fig. 12. Effect of jump-in-strain-rate at 643 K from 3.2×10^{-3} s^{-1} to 3.2×10^{-2} s^{-1}. The strain at which the jump took place is 0.126.

1 in the homogeneous regime. Recently, a model was proposed using the concept of fictive stress [19] in which the uniaxial stress rate is described using a simple Maxwell model,

$$\frac{d\sigma}{dt} = E\frac{d\varepsilon}{dt} - \frac{\sigma}{\lambda}, \tag{3}$$

where E is the Young's modulus which is a function of temperature, ε is the strain, σ is the stress and λ is the relaxation time. If the relaxation time λ is only a function of temperature, then for a given temperature and strain rate, the general solution for stress is a monotonically increasing function reaching a steady state after a strain of approximately$\varepsilon = \dot{\varepsilon}\lambda$. However, the actual response of metallic glasses does not always exhibit such a tendency.

In the steady state regime, the flow stress can be expressed as the ratio of the viscosity (η) to the relaxation time (λ). Since the steady state flow stress is a constant for a given temperature, it is reasonable to assume that the relaxation time scales linearly with viscosity, i.e., $\eta/\eta_N = \lambda/\lambda_N$. If λ/λ_N(or η/η_N) is plotted as a function of $\sigma_{flow}/\sigma*$ as shown in Fig. 13, where $\sigma*$ is a "maximum" stress used to normalize the steady state flow stress σ_{flow}, the flow stress can be described using a functional form, $\sigma_{flow}/\sigma* = f(\lambda/\lambda_N)$. Instead of using the free volume concept, one can then use the structural relaxation time λ_{relax} to represent the change in the microstructure of the material. Once a steady state flow stress is given, a corresponding λ_{relax} can be obtained by simply assuming $\lambda_{relax} \approx \lambda$. This concept can be further extended to the transient response of the material subjected to loading. A fictive stress σ_{fic}[19] and a transient relaxation time λ_{tra} are introduced satisfying the same relation as for the flow stress, $\sigma_{fic}/\sigma* = f(\lambda_{tra}/\lambda_N)$. The fictive stress is assumed to be dependent on both actual stress and the transient relaxation time λ_{tra} through the following kinetic relation,

$$\frac{d\sigma_{fic}}{dt} = \frac{\sigma - \sigma_{fic}}{\lambda_{tra}}. \tag{4}$$

It is easy to see from Eq. (4) that at steady state $\dot{\sigma}_{fic} = 0$, and, the fictive stress is equal to the actual steady state flow stress, consistent with the previous assumption. An empirical relation for the transient relaxation time based on the best fit to the experimental data is as follows,

$$\frac{\lambda_{tra}}{\lambda_N} = \left(1 - \frac{\sigma_{fic}}{\sigma*}\right) \Big/ \left(1 + \frac{\sigma_{fic}}{\sigma*}\right). \tag{5}$$

Consequently,

$$\frac{d\lambda_{tra}}{dt} = \frac{-2 \quad \lambda_N d\sigma_f}{(1 + \lambda_f/\lambda_N)^2 \sigma^* \, dt}. \tag{6}$$

This simple model can now be used to describe the deformation behavior of a metallic glass in its homogeneous regime. Figs. 14 and 15 show the comparison of model predictions with experimental data at various temperatures and strain rates. Young's modulus was chosen as a function of temperature and rate of deformation in accordance with the experimental results. The initial relaxation time λ_N and the reference stress $\sigma*$ are also based on the experimental results and the values used in the model are indicated in the figure captions. For the initial relaxation time λ_N in the model, the relaxation time determined from the experiments as depicted in Fig. 6 was used and the resulting predictions were not in agreement with the experimentally obtained stress-strain curves. It was found that the experimental results were best modeled by scaling the relaxation time in Fig. 6 by a factor of 1/3–1/5 while keeping the relaxation time as a function of temperature, which is in accordance with the scaling suggested by Kato et al. [19] in their study.

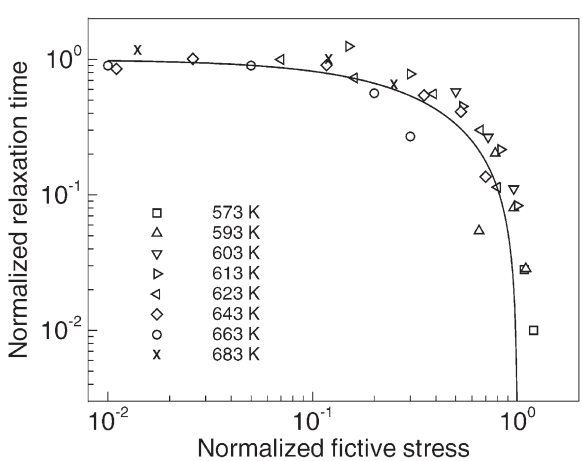

Fig. 13. Normalized relaxation time λ/λ_N(or η/η_N) as a function of normalized fictive stress $\sigma_{flow}/\sigma*$.

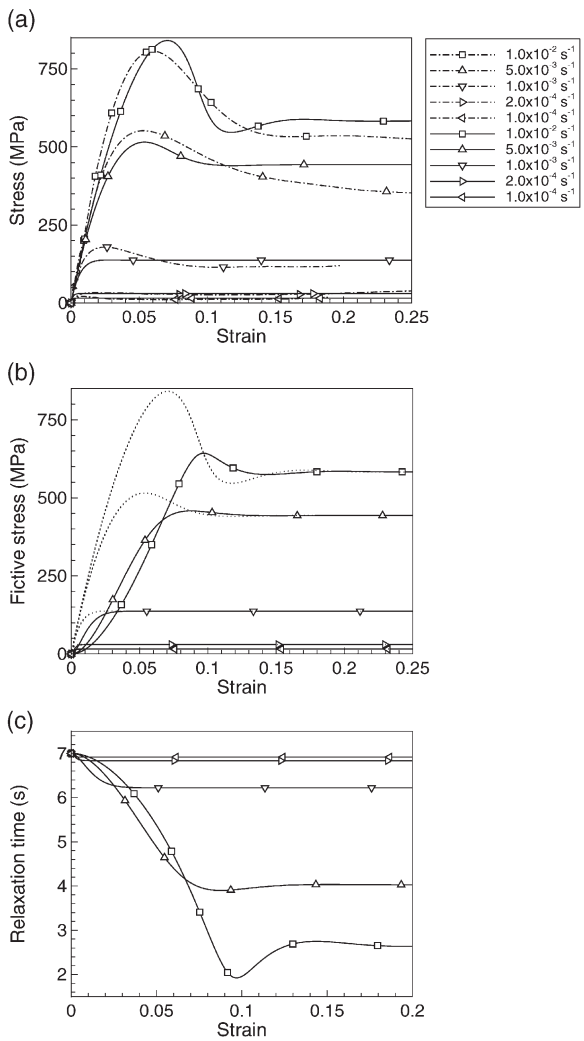

Fig. 14. Model predictions at T=643 K based on the fictive stress model, E=22 GPa, $\sigma*$=650 MPa, λ_N=7 s: stress-strain curves with dashed lines correspond to the experimental data and the ones with solid lines correspond to the model prediction.

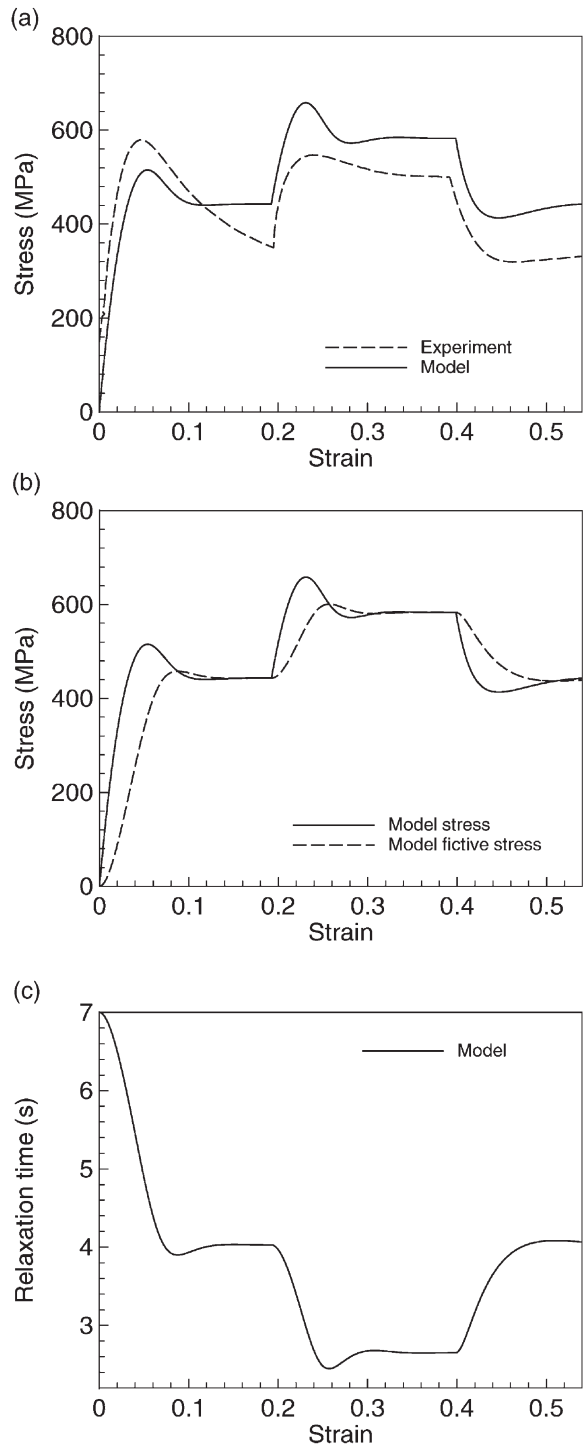

Fig. 15. Model predictions of the effect of jump in strain rate at T=643 K based on the fictive stress model. The strain rate jumped from 5.0×10^{-3} s^{-1} to 1.0×10^{-2} s^{-1} and then back to 5.0×10^{-3} s^{-1}: (a) stress-strain curves with dashed lines correspond to the experimental data and the ones with solid lines corresponding to the model prediction; (b) fictive stress (solid line) and stress (dotted line) as a function of strain; and (c) relaxation time as a function of strain.

At a temperature of 643 K, five typical stress-strain curves corresponding to strain rates of 1×10^{-4} s^{-1}, 2×10^{-4} s^{-1}, 1×10^{-3} s^{-1}, 5×10^{-3} s^{-1} and 1×10^{-2} s^{-1} are shown in Fig. 14(a). The predicted stress-strain curves agree reasonably well with the experimental results (Fig. 12(c)), as shown in Fig. 14(a). The stress peaks and the slopes at the early stage of the deformation also match reasonably well with the experimental data. At higher strain rates, the slopes of the descending part after the peaks seem to be steeper than what was observed in the experiments, and higher levels of steady state flow stress are predicted. The transition from Newtonian to non-Newtonian flow appears at a strain rate higher than 1×10^{-3} s^{-1}, which is close to the value observed in the experiments (Fig. 11). The transition can be demonstrated again by looking at the relaxation time-strain relationship as shown in Fig. 14(c). Clearly, at the two smallest strain rates, the corresponding transient relaxation time remains almost a constant, with very limited drop before the corresponding steady state stress levels off. At the strain rate of 1×10^{-3} s^{-1}, a small stress overshoot emerges, accompanied by a pronounced decrease in the relaxation time of more than 10%. As the strain rate increases, the decrease in the relaxation time becomes so significant that oscillations are observed in the stress-strain curve. The fictive stress, on the other hand, serves as a bridge to link the transient relaxation time and the deformation. The plot in Fig. 14(b) illustrates the variations of the fictive stress with respect to strain. It is interesting that the variation of the free volume has a similar tendency compared with that of the fictive stress: both lag behind the actual stress of the material, which suggests that there might exist a correlation between the two variables. Consequently, in the context of the present phenomenological model, one can think of fictive stress as another empirical function of the free volume.

As shown earlier, a jump in the strain rate has a pronounced effect on the stress-strain response of Vitreloy 1. The present fictive stress model can also reproduce this effect. Such high strain rate sensitivity in the low strain rate regime is not generally observed in crystalline metallic materials. Fig. 15 shows the model predictions and the experimental data for Vitreloy 1 at 643 K subjected to a sequence of jumps in strain rate. An initial strain rate of $5.0 \times 10^{-3}s^{-1}$ was applied to the specimen, followed by a higher strain rate of 1.0×10^{-2} s^{-1}. At a strain of around 0.4, the strain rate was reset to its original value, $5.0 \times 10^{-3}s^{-1}$. The stress jumps observed in the experiment are reproducible by the model. The model predictions show that the final steady state flow stress reaches a value close to the steady state flow stress at the initial strain rate of $5.0 \times 10^{-3}s^{-1}$, indicating that the intermediate deformation history has no significant effect on the steady state stress. Also, the change of fictive stress at the strain where the strain rate jumps is quite slow and smooth compared with that of the actual stress. The relaxation time begins to decrease at a higher rate after the jump in strain rate, and stress undershoot is clearly observed in the plot.

6. Conclusions

The uniaxial stress-strain behavior of a bulk metallic glass, namely Vitreloy 1 ($Zr_{41.2}Ti_{13.8}Cu_{12.5}Ni_{10}Be_{22.5}$) was investigated experimentally over a wide range of strain rates as well as temperatures. The following conclusions are drawn from this investigation:

1. The deformation of Vitreloy 1 bulk metallic glass is very sensitive to loading rate and temperature near and above its glass transition, 623 K, i.e., in the supercooled liquid region. Quasi-static experiments revealed that Vitreloy 1 exhibits high-strain-rate sensitivity over the temperature range of 573–683 K, especially in the supercooled liquid region. However, under dynamic loading conditions, 10^2 s^{-1} to 10^3 s^{-1}, the strain rate effect is insignificant. At temperatures below 573 K, the material has high strength, exhibiting less strain rate sensitivity compared with the high temperature regime. At room temperature, Vitreloy 1 is virtually rate insensitive over a broad range of strain rates, up to 10^3 s^{-1}, which is consistent with the earlier observation [11].
2. The deformation of bulk metallic glasses can be

divided into three modes, namely, Newtonian flow, non-Newtonian flow, and shear localization. It is found that homogeneous deformation in Vitreloy 1 can be achieved at a strain rate nominally higher than 1 s^{-1} in the high temperature side of its supercooled liquid region. The non-Newtonian viscosity of Vitreloy 1 is substantially smaller than its corresponding Newtonian viscosity in this range of temperatures. Such a trend can be well expressed using a master curve which describes normalized viscosity as a function of normalized strain rate. The studies of stress overshoot and relaxation also revealed that the flow of Vitreloy 1 is very sensitive in the supercooled liquid region and quasi-static strain rates.

3. A simple modified Maxwell viscoelastic model, originally proposed by Kato et al. [19], was employed to understand the flow characteristics of metallic glass. The relaxation time correlated well with a "fictive" stress which is the conceptual extension of the steady state flow stress in the transient deformation regime and was no longer assumed constant but varied during deformation. This model is able to capture the basic characteristics of the stress-strain curves, as well as the jump-in-strain rate effects of Vitreloy 1 reasonably well. It also suggests that the variation of the "fictive" stress likely represents the trend of the free volume variation with inelastic deformation.
4. Due to its extreme high strength and light weight, Vitreloy 1 has been produced in large quantities for structural applications using high-pressure injection casting. In order to obtain high quality material, attention needs to be focused on avoiding inhomogeneous shear localization, phase separation and crystallization. Since Vitreloy 1 is highly metastable with a large supercooled liquid region to suppress crystal formation, preventing inhomogeneous shear localization is of major concern in deformation processing and casting. An important issue is the choice of processing conditions for bulk metallic glasses to avoid shear localization and yet achieve a high rate of productivity. From the current investigation, it is evident that the processing speed (or pressure) must be set such that the corresponding effective strain rate is smaller than the critical effective strain rate of inhomogeneous deformation predetermined at the mold temperature. In this respect, the data for Vitreloy 1 in Fig. 11 provides the necessary design data for optimal processing conditions. Casting process should be controlled within the homogeneous deformation region away from the boundary of shear localization in order to produce high quality material.

Acknowledgements

This work was sponsored by the Structural Amorphous Metals Program of the Defense Advanced Research Projects Agency (DARPA), under ARO Contract No. DAAD19-01-1-0525, and, in part by the Center for Science and Engineering of Materials at the California Institute of Technology through a grant from the MRSEC program of the National Science Foundation, which are gratefully acknowledged.

References

[1] Johnson WL. Metastable phases. In: Westbrook JH, Fleischer RL, editors. Intermetallic compounds, vol. 1. New York: Wiley; 1994. p. 687.
[2] Inoue A. Bulk amorphous alloys: preparation and functional characteristics. Uetikon-Zuerich, Switzerland: Trans Tech Publications, 1998.
[3] Klement WJ, Willens RH, Duwez P. Nature 1960;187:869.
[4] Chen HS. Mater Sci Eng 1976;25:59.
[5] Chen HS. J Appl Phys 1978;49:3289.
[6] Inoue A, Ohtera K, Kita K, Masumoto T. Jpn J Appl Phys 1988;27:L2248.
[7] Peker A, Johnson WL. Appl Phys Lett 1993;63:2342.
[8] Johnson WL. Mater Sci Forum 1996;225-227:35.
[9] Johnson WL. Solid State Mater Sci 1996;1:383.
[10] Bruck HA, Christman T, Rosakis AJ, Johnson WL. Scripta Metall 1994;30:429.
[11] Bruck HA, Rosakis AJ, Johnson WL. J Mater Res 1996;11:503.
[12] Kim YJ, Busch R, Johnson WL, Rulison AJ, Rhim WK. Appl Phys Lett 1994;65:2136.
[13] Busch R, Kim YJ, Johnson WL. J Appl Phys 1995;77:4039.
[14] Masuhr A, Busch R, Johnson WL. J Non-Cryst Solids Part 2 1999;252:566.

[15] Masuhr A, Waniuk TA, Busch R, Johnson WL. Phys Rev Lett 1999;82:2290.
[16] Kawamura Y, Shibata T, Inoue A, Masumoto T. Appl Phys Lett 1996;69:1208.
[17] Kawamura Y, Nakamura T, Inoue A, Masumoto T. Mater Trans JIM 1999;40:794.
[18] Kato H, Kawamura Y, Chen HS, Inoue A. Jpn J Appl Phys 2000;39:5184.
[19] Kato H, Kawamura Y, Inoue A, Chen HS. Appl Phys Lett 1998;73:3665.
[20] Nieh TG, Wadsworth J, Liu CT, Ohkubo T, Hirotsu Y. Acta Mat 2001;49:2887.
[21] Argon AS. Acta Metall 1979;27:47.
[22] Argon AS, Shi LT. Acta Metall 1983;31:499.
[23] Megusar J, Argon AS, Grant NJ. Mater Sci Eng 1979;38:63.
[24] Spaepen F. Acta Metall 1977;25:407.
[25] Steif PS, Spaepen F, Hutchinson JW. Acta Metall 1982;30:447.
[26] Khonik VA. Phys Status Solidi 2000;A177:173.
[27] Duine PA, Sietsma J, van den Beukel A. Acta Metall 1992;40:743.
[28] de Hey P, Sietsma J, van den Beukel A. Mater Sci Eng 1997;A226-228:336.
[29] de Hey P, Sietsma J, van den Beukel A. Acta Mater 1998;46:5873.
[30] van Aken B, de Hey P, Sietsma J. Mater Sci Eng 2000;A278:247.
[31] Kato H, Kawamura Y, Inoue A, Chen HS. Mater Trans JIM 2000;41:1202.
[32] Chen HS, Kato H, Inoue A. Jpn J Appl Phys Part 1 2000;39:1808.
[33] Busch R, Kim YJ, Johnson WL, Rulison AJ, Rhim WK, Isheim D. Appl Phys Lett 1995;66:3111.
[34] Fecht HJ. Mater Trans JIM 1995;36:777.
[35] Conner D. Ph.D. Thesis. California Institute of Technology, 1998.
[36] Owen DM, Rosakis AJ, Johnson WL. Dynamic failure mechanisms in beryllium bearing bulk metallic glasses. In: Johnson WL, Inoue A, Liu CT, editors. MRS Symposium Proceedings Vol. 554. Bulk Metallic Glasses. Warrendale, Pennsylvania: Materials Research Society; 1999.
[37] Lu J. Ph.D. Thesis. California Institute of Technology, 2002.
[38] Kolsky H. Proc R Soc Lond 1949;B62:676.
[39] Gray III GT. Classic split-Hopkinson pressure bar testing. In: Medlin D, Kuhn H, editors. ASM handbook, vol. 8. Materials Park (OH): ASM International; 2000. p. 462.
[40] Subhash G, Ravichandran G. Split Hopkisnon bar testing of ceramics. In: Medlin D, Kuhn H, editors. ASM handbook, vol. 8. Materials Park (OH): ASM International; 2000. p. 497.
[41] Chen W, Ravichandran G. J Mech Phys Solid 1997;45:1303.
[42] Matsuka S. Relaxation phenomena in polymers. New York: Hanser Publishers, 1992.
[43] Scherer GW. Relaxation in glass and composites. Malabar(FL): Krieger Publishing, 1992.
[44] Gupta RK. Polymer and composite rheology. New York: Marcel Dekker, 2000.
[45] Grest GS, Cohen MH. Adv Chem Phys 1981;48:455.